Environ. Sci. Technol. **2004**, *38,* 5712−5720

Receptor Modeling of Toronto $PM_{2.5}$ Characterized by Aerosol Laser Ablation Mass Spectrometry

SANDY OWEGA, BADI-UZ-ZAMAN KHAN, RYAN D'SOUZA, GREG J. EVANS,* MIKE FILA, AND ROBERT E. JERVIS

Department of Chemical Engineering and Applied Chemistry, University of Toronto, 200 College Street, Toronto, Ontario M5S 3E5, Canada

Urban Toronto fine particulate matter ($PM_{2.5}$) was physically and chemically characterized by online aerosol laser ablation mass spectrometry (LAMS) between January 2002 and February 2003. The mass spectra from the analysis of individual aerosol particles were classified according to chemical composition by a neural network approach called adaptive resonance theory (ART-2a). Temporal trends of the hourly analysis rate of over 120 different particles types were constructed and subjected to positive matrix factorization (PMF). This receptor modeling technique enabled the identification of nine distinct emission sources responsible for these particle types: biogenic, mixed crustal, organic nitrate, construction dust, Toronto soil/road salt, secondary salt, wood burning, intercontinental dust, and an unknown source of aluminum fluoride dust. Episodic events occurred with the wood burning, intercontinental dust, and unknown dust sources. This is the first paper reporting the application of PMF to single-particle spectral data.

Introduction

Atmospheric aerosol data is especially problematic to characterize because it is influenced by multiple sources whose contributions are variable over time. Additionally, each of these sources may have markers that are only present in sparse quantities. The need for receptor modeling and source apportionment has driven the application of the science of factor analysis in this field, and this has produced several different tools and general solvers, such as principal component analysis (PCA), positive matrix factorization (PMF), and the multilinear engine (ME), sensitive to the type and context of the data being analyzed.

Factor analysis is a multivariate statistical technique commonly used in environmental studies to deduce sources from data taken at receptor sites (*1*). Various methods for factor analysis have been proposed that are based on principles of correlation or covariance like PCA. However, these techniques are subject to several inconsistencies, especially rotational ambiguity or the lack of uniqueness of solution (*1*). An important new approach to factor analysis, PMF, recognizes factor analysis as an explicit least-squares problem (*1*). PMF has been chosen for receptor modeling in this work as it reduces rotational ambiguity in results, allows the inclusion of missing or below detection limit values, generates nonnegative source profiles. and has been successfully used to represent environmental data (*2*−*7*).

PMF relies on the accuracy of error estimates to produce reliable results and uses the estimates of the error in the data to provide optimal point-by-point weighting. This is particularly important when less robust data sets, containing many missing or below detection limit values that could have the ability to define real sources or even be markers, are to be used in the analysis. The method has been applied to the apportionment of airborne particles in a number of locations (*2*−*7*). Applications of PMF, which has recently been used in the United States to identify local aerosol sources (*2*, *3*, *8*), form an expanding body of literature.

Depending on the geographic location, unique types of factors could be isolated via PMF. For example, heavy-duty diesel characterized by high elemental and organic carbon was observed by use of PMF at Phoenix, AZ (*3*) but not at Washington, DC (*2*, *8*). Nevertheless, some factors, like oil combustion typified by Ni and V and soil represented by Al, Ca, Fe, K, Si, and Ti, are resolved by PMF at many locations (*2*, *3*, *8*), and the number of factors in the northeastern United States, near Toronto, has ranged between 8 and 11 (*2*, *8*).

Previous PMF studies, including the examples cited above, have mostly been performed with elemental and ionic species concentrations determined through analysis of daily filter samples (*2*−*7*). This paper describes the first application of PMF to single-particle aerosol data classified into particle types. The data differed from previous results interpreted by PMF in two significant ways. First, particle types were used instead of elements; second, hourly "hit rates" were used instead of daily resolved concentrations. The use of PMF also differentiates the study from previous source apportionment interpretations to TOFMS data (*9*, *10*). The application of PMF allowed particle types believed to originate from a number of different sources to be apportioned between these sources. Additionally, the treatment of a large number of zeros in the input data matrix was unprecedented and, upon analysis of prior publications, there was no consistent technique devised to determine the number of factors. The first complication was addressed with development of a technique to calculate the input error matrix for PMF, even though no prior information regarding class-specific detection limits was available. For the second complication, the analyst's judgment was employed; that is, the number of factors chosen was that which could be physically interpreted and explained by known source patterns. A detailed solution to the first complication in the case of known standard materials will be described elsewhere, while the second is addressed in this work. Finally, the present work also attempted to extend prior work using filter-based measurements and achieve a more comprehensive representation of particulate matter in Toronto. Size distribution has been useful in determining sources (*11*−*13*) and could be used in the future as an additional discriminating aspect in such factor analysis techniques.

Methodology

Aerosol Laser Ablation Mass Spectrometry of Ambient Particulate Matter. Urban Toronto $PM_{2.5}$ was physically and chemically characterized by an aerosol LAMS between January 14, 2002, and February 5, 2003. Operation and sampling procedures for the aerosol LAMS have been previously documented (*14*). In brief, aerosol particles were concentrated outside the instrument before passing into the LAMS inlet. Gas surrounding the particles was removed at the inlet, generating a particle beam. Single particles traveled

* Corresponding author phone: (416)978-1821; fax: (416)978-8605; e-mail: evansg@chem-eng.utoronto.ca.

10.1021/es035177i CCC: $27.50
Published on Web 09/29/2004

along the particle beam trajectory to eventually intersect two He−Ne laser light paths separated by a known distance. The light scattered by the particle was recorded with two photomultiplier tubes (PMT), and the time between these electric pulses was converted to an aerodynamic equivalent diameter. In addition, this time controlled the firing of a Big Sky Nd:YAG laser (266 nm) (Bozeman, MT) to ablate the particle in the ion source chamber of a time-of-flight mass spectrometer (TOFMS). Once the particle was ablated, the ions were accelerated with electric fields into a field-free drift tube. The ions entered a reflectron, traveled back through the field-free drift tube, and struck a microchannel plate (MCP) detector. The signal from the MCP was recorded with a 500 MHz LeCroy Model LC334A digital storage oscilloscope (DSO) (Chestnut Ridge, USA). A computer was coupled to the oscilloscope to transfer each spectrum in real time. The spectrum from the computer was calibrated with software and stored for further data analysis.

Creation and Selection of ART-2a Classes Entire Sampling Period. The aerosol LAMS was capable of generating spectra for cations and anions by means of polarity reversal on the ion acceleration grid every 10 min of sampling. Approximately 170 000 positive and 60 000 negative mass spectra were generated by the particles sampled during the 13-month period. The measured intensities of selected ions in each spectrum were first converted to a standardized (zero mean and unit standard deviation) intensity variable. Our previous research (*15*) developed a selected list of cations and anions that assisted in the chemical classification of spectra. The selected cations were $^{12}C_n$ ($n = 1-5$), $^{18}NH_4$, ^{23}Na, ^{24}Mg, ^{27}Al, ^{30}NO, ^{39}K, ^{40}Ca, ^{41}K, ^{48}Ti, ^{51}V, ^{55}Mn, $^{56}Fe/^{56}CaO$, $^{58}C_3H_8N$, $^{59}C_3H_9N$, ^{63}Cu, $^{64}Zn/^{64}TiO$, $^{81}Na_2Cl$, ^{138}Ba, ^{208}Pb, $^{213}K_3SO_4$, and $^{215}K_3SO_4$. The selected anions were $^{12}C_n$ ($n = 1, 2, 4-6$), ^{16}O, ^{17}OH, ^{19}F, $^{26}CN/^{26}C_2H_2$, ^{35}Cl, ^{37}Cl, $^{46}NO_2$, $^{59}C_3H_7O$, $^{60}SiO_2$, $^{62}NO_3$, $^{76}SiO_3$, $^{79}PO_3$, $^{81}HSO_3$, $^{93}Cl(NaCl)$, and $^{97}HSO_4$. The remaining m/z values were found to appear infrequently in the LAMS spectra.

The conventional neural network ART 2a performed the classification of the standardized data in order to assign each mass spectrum generated during the sampling period to either a positive or negative particle type, depending on the polarity of the spectrum. The vigilance factor (similarity criterion), the learning rate (step size), and the number of epochs (iterations) of this network have previously been empirically determined. A choice of 0.4 for the vigilance factor prevented both the overlapping between,and the segregation of, distinct particle types. While the choice of vigilance factor is lower than that used in previous studies, it is important to realize that the present work used unit vectors with negative elements, and thus, the range of possible vigilance factors lied between −1 and 1. Similarly, a learning rate of 6% and 10 epochs prevented misclassifications from exceeding 5%. In this manner, 62 positive and 62 negative particle types were generated.

It is worth noting that the sensitivity of the LAMS likely varied substantially for the different particle types but this could not be determined. In particular, high sensitivity to alkali metals has been noted (*16*). Suess and Prather (*16*) note that laser power (related to the lattice energy and/or ionization potential of a species), spot size, and absorption characteristics of the sample matrix and individual species present all affect the sensitivity of LAMS. Thus, the observed distribution of particle types did not reflect their actual distribution. However, this ablation approach was retained due to extensive advantages such as the online analysis of atmospheric aerosol and especially its nonvolatile components (*16*). Furthermore, the sensitivity issue is not a limitation to identifying sources by PMF but does impact on determining the overall apportionment.

Since the intensities at the selected m/z values in the input data set were standardized to a mean of 0 and standard deviation of 1, the naming of the particle types generated by ART-2a was achieved by recording the selected m/z values that displayed significant positive intensities after standardization. The name assigned to a particle type thus represented the ion associated with the m/z value observed with an above average intensity. When more than one selected m/z value displayed positive intensities after standardization, a dash separated the ions associated with the above average intensity m/z values. In this special case, the ions were ranked in descending order. For example, the positive particle type named as ^{39}K exhibited an above average intensity at an m/z of 39. However, a positive particle type named $^{39}K-^{12}C$ displayed both potassium and carbon, with the intensity of potassium more positive than that of carbon at their respective m/z. Note that this approach allows one to also find m/z values that are present in less than average amounts and thus do not really contribute to the spectrum on an overall basis. We believe that recognizing the components that are comparatively absent can complement knowing the key components of a particle type.

The number of particle types was tallied on an hourly basis, and then 5-hour averaged to illustrate the temporal variation of that particle type. Typically, data sets used in PMF analysis range between 1 and 5 years, providing between 365 and 1900 data points to define a temporal trend for one chemical concentration by filter-based measurements. The temporal trend for each particle type consisted of the number of particles of that type detected during each hour of the 9285 h of sampling, smoothed with a 5-h moving average. For many particle types, this value was frequently zero. Hence, methods to estimate the minimum detection limit and the error on the data set were next performed to allow PMF to accommodate the large number of zeros in the data set. Note that while sizing information was available for each spectrum, it was not used because the dataset was already very large (9285 rows by 124 columns) and computational difficulty was obvious. Furthermore, such a subdivision would increase the number of zeros in the dataset. It was, however, interesting to note that while the median size of particles associated with crustal sources hovered around 1.3 μm, that of particles associated with secondary sources was approximately 0.9 μm.

Efforts are currently underway to incorporate sizing information into the PMF analysis, as demonstrated by Allen et al. (*17*), who scaled particles in a given size range by the inlet efficiency in that range and then compared with the actual size distribution data. Unfortunately, the latter was not available for the sampling duration. Future studies are expected to consider this information. For the present work, the various emission sources were identified by their chemical composition and via diurnal and weekend/weekday behavior.

Operating Principle, Estimation of Errors, and Optimal Choice of Factors in PMF. The operation of PMF has been detailed elsewhere (*1*, *2*). In this work, PMF solved for the temporal trends of emission sources and their constituent particle types, termed source profiles, by using the temporal trends of the particle types and associated error estimates. Since no error information on the temporal variation of each particle type existed, an objective estimation of errors was required. This was achieved by calculating the fraction of zeros in the hourly hit data for each particle type to determine its detection limit. The detection limit for a particle type was defined as the product of the fraction of its zero-valued points with 0.2, since one hit over an averaging time of 5 h was the smallest possible nonzero observation rate. Hence, a frequently observed particle type was assigned a lower detection limit than a less frequently observed one. The product of this detection limit with a constant, a standard technique (*2*),

provided the error estimate at the zero-valued points. This constant was set at 4 in this work. The zero-valued points were themselves replaced by the detection limit. The error at the nonzero points in a given temporal trend was then approximated with their corresponding standard deviations. An exponential decay function was used to scale down the error on sharp increases in the hit rate of a given particle type. This function highlighted these temporal peaks, which contained important information that would be lost if only the standard deviation was used as an error estimate. Note that assigning arbitrarily chosen weights to scale down errors for certain species, as reported elsewhere (*2*), is a less objective approach than one based on the temporal trend of a particle type.

There is no exact rule for judging the optimal number of PMF factors (*18*). The solution can nonetheless be chosen subjectively if the calculated source profiles can be reconciled with known emission sources (*19*, *20*). Hence, PMF solutions with factorization ranks 3−15 were obtained. It was noted that an eight-factor solution failed to separate two episodic dust sources. Furthermore, a 10-factor solution separated a road salt source from its crustal contaminants. Even though this was desirable, the sensitivity of the LAMS towards road salt was known to be poor. Thus, a nine-factor solution was chosen. It should also be noted that although there were more positive spectra than negative, this did not bias the PMF analysis, as the emphasis PMF placed on any component depended on the relative rather than absolute variation within the associated time series.

Finally, while built-in tools for assessing rotational ambiguity like FPEAK were tested, no significant improvements in the source profiles were observed. Furthermore, Paatero et al. (*21*) note that there is no justification for choosing a nonzero FPEAK value if specific patterns of zero-valued elements in either the source profile or source temporal trend or both are not known a priori. In our work, we did not know of the existence of sources such as organic nitrate in summertime and road salt contaminated with crustal matter in the wintertime beforehand. For these reasons, the FPEAK value was set at zero for this work.

Results and Discussion

Identification of Crustal Sources during Nonepisodic Events with PMF Receptor Modeling. Figure 1A,B illustrates the positive and negative source profiles of the three crustal factors produced by PMF, while Figure 1C displays their temporal trends. Weighted multiple regression coefficients were used to scale the source profiles and time series in Figures 1, 3, and 4. Note that the fraction of positive and negative particle types, for a particular factor, will sum together to unity. The first factor in Figure 1 was labeled as a construction dust source. Crustal metallic positive particle types such as calcium, calcium oxide, sodium, potassium, and iron were observed with their negative organic and chloride counterparts. The exceptionally high levels of calcium and calcium oxide suggest cement constituents mixed with Toronto soil and are consistent with the results from other studies (*22*, *23*). This source was primarily observed in the winter season of 2002 and 2003. Coincidentally, at the beginning of October, construction near the receptor site commenced. Interesting features about this source included sodium chloride, or road salt, probably transferred by the construction vehicles on the adjoining road during the winter, explaining the chloride mixed with the negative Toronto soil constituents. In addition, inorganic chemical markers of soil like barium, titanium, and iron were also observed (*23*). These assertions were supported by the marked enhancement of daytime and weekday levels of this source over nighttime and weekend levels (see Figure 2).

The second factor was identified as a Toronto soil/road salt source and was most apparent in the winter season. The dominant positive particle type of this source was primarily sodium chloride, exhibited as sodium and sodium chloride, with the similar negative particle types. A local source like the road salt spread to combat the winter ice on streets and sidewalks close to the receptor site is proposed. Barium, magnesium, titanium, and iron particle types were also observed, suggesting a crustal component to this source. This indicates that this source was road salt contaminated by local Toronto soil and road dust. It is worth noting that the sensitivity of the LAMS for pure road salt is very low. It is believed that the presence of a contaminant is required in salt particles to facilitate their detection. Hence, the presence of the soil on the road salt particles appears to have enhanced their observation. Similar to the construction dust source, diurnal behavior was clearly observed (see Figure 2), indicating an anthropogenic source.

The last factor in Figure 1 was labeled as a mixed crustal source. Some bias toward the spring season was observed in its temporal trend, and according to its source profile from PMF, the most prominent positive particle types observed were calcium and other crustal metals, although organic contributions were also observed. The corresponding negative particle types observed were oxides, silicates, nitrates, and sulfates. Its mixed nature was indicated by the similar contributions of several negative particle types to its source profile. It initially seemed that this source was a mixture of regional soil and fly ash materials. This was because incinerator, coal fly ash, and soil materials characterized previously by our aerosol LAMS exhibited these particle types (*14*). Furthermore, lead was also observed in this source, which is in agreement with other publications (*23*). Crustal components such as aluminum, iron, and silicates are also constituents of coal ash and are recycled from waste streams produced from coal burning (*24*). However, the diurnal and weekday/weekend trends of this source (shown in Figure 2) suggest an anthropogenic effect in this source, coinciding with the morning rush hour and sunrise. It is thus very likely that this source was a mixture of local soil and resuspended road dust.

Identification of Secondary Sources during Nonepisodic Events with PMF Receptor Modeling. The positive and negative source profiles of the three secondary nonepisodic factors generated by PMF are displayed in Figure 3A,B. The corresponding temporal trends are illustrated in Figure 3C. The label "secondary" was used to describe the presence of secondary components on the particles even though some may have had a primary core. The first factor, labeled as a biogenic source, exhibited organics and crustal positive particles coated with amine compounds. Counteranionic particles of nitrates and sulfates were observed in this factor, indicating secondary gas−particle surface reactions. Amine compounds had previously been observed in Toronto during the winter season (*25*) and were strongly evident during the winter between January 2002 and February 2002. Nitrates have been identified as the counterion for the positive amines (*26*). It is believed that this source was not observed in the following winter due to its greater snowfall suppressing the emission of the amines. Volatile amines outgassed from municipal sewer wastewater in the city or from agricultural animal operations are suggested as possible sources (*27*). Note that PMF solutions with over 9 factors failed to split this source, and it is thus believed to be the only biogenic identifiable.

The second factor in Figure 3 was identified as a secondary salt source. Similar to the Toronto soil/road salt source, the temporal trend demonstrated higher concentrations during the winter than the summer. However, no diurnal trend was observed. The dominant positive and negative particle types

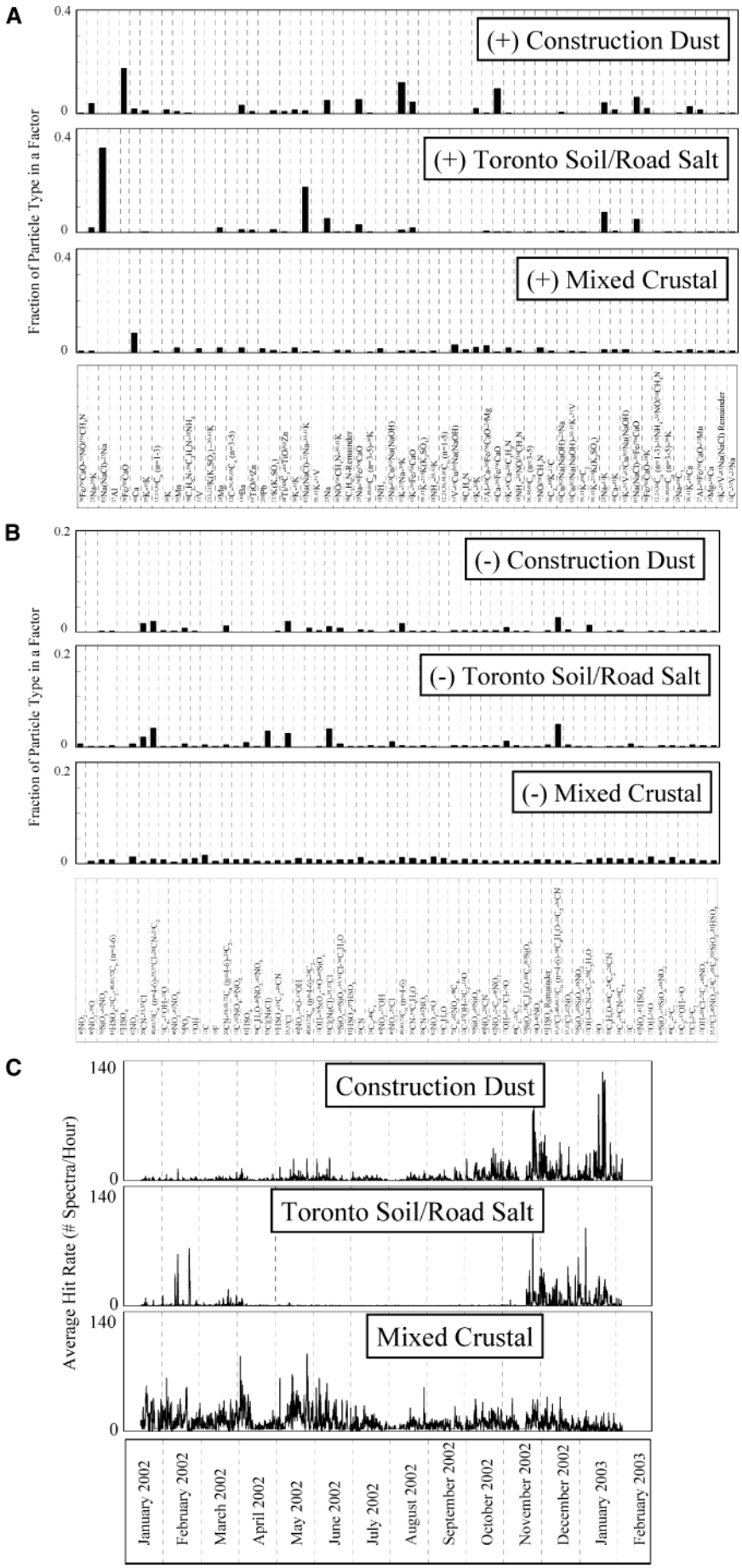

FIGURE 1. (A) Positive and (B) negative crustal source profiles and (C) crustal temporal trends for nonepisodic events.

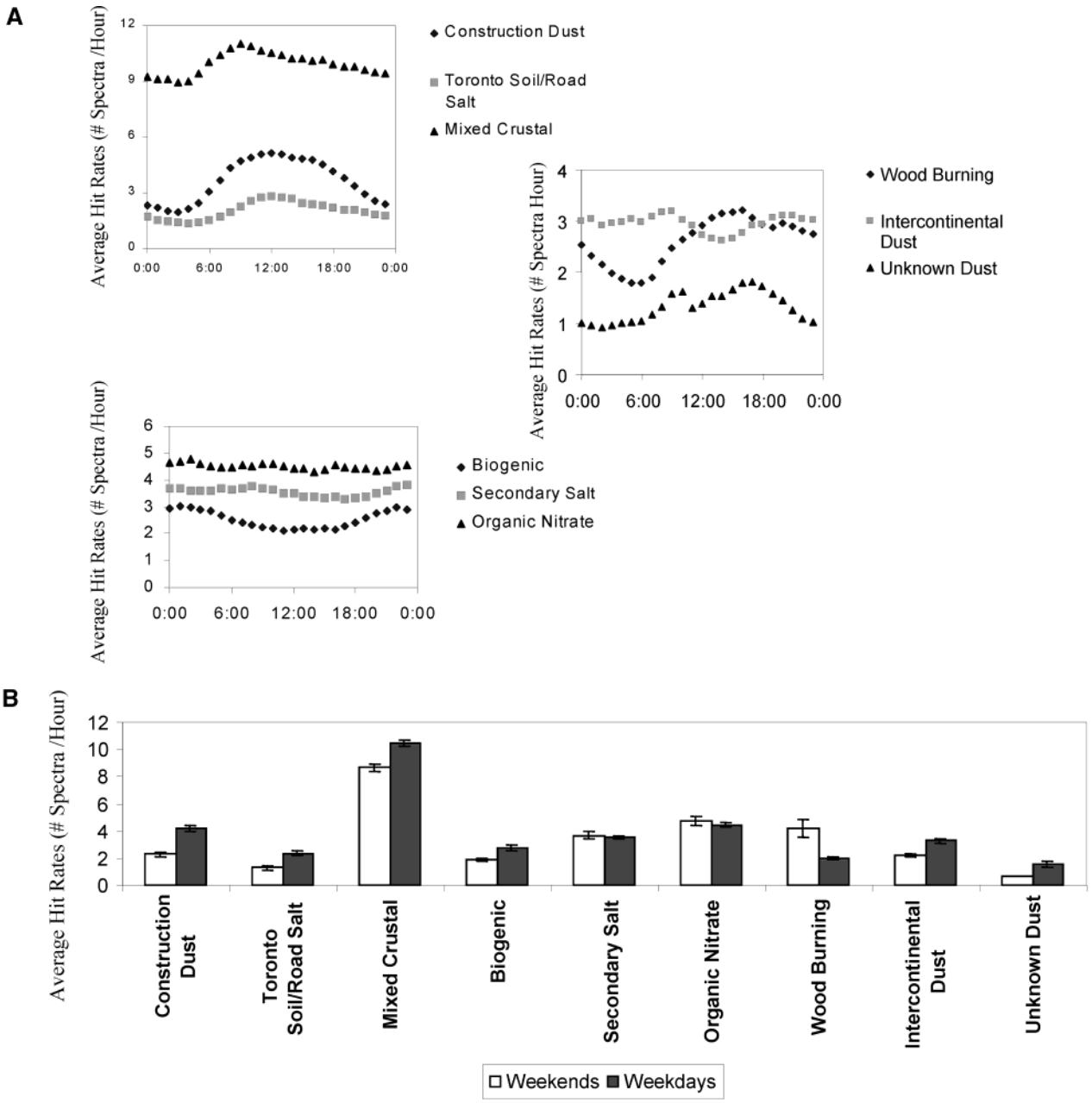

FIGURE 2. (A) Diurnal and (B) weekend/weekday behavior of PMF sources. Error bars represent 95% confidence interval on each mean value.

of this source were primarily sodium hydroxide and nitrate, respectively. We propose that salt particles may have undergone nitrification through reaction with gaseous nitric acid to form sodium nitrate particles and gaseous hydrochloric acid (*28*), the equilibrium constant for this reaction increasing as the temperature decreased (*29*). Nitrate is typically produced through the secondary transformation of particles via gas−particle surface reactions with NO_x (*30*). We speculate that the observed sodium hydroxide was formed via the conversion of sodium nitrate to gaseous nitric acid in the presence of water from the snow. These reactions may explain why this source was observed during the Toronto winter season. It is unclear if the origin of the sodium chloride in the particles was oceanic or road salt.

The third factor was labeled as an organic nitrate source. It exhibited a temporal trend with some similarities to that of the mixed crustal source with a summer season bias, as well as some manganese. The positive potassium and carbon cluster particle types displayed the largest contribution. The carbon cluster particle types associated with this source were only minor components in the profiles of the other emission sources, while the reason for the presence of the potassium particles is not known. These particles persisted in the profile for high FPEAK values also. The corresponding negative particle types that were observed in this source were similar to those observed in the mixed crustal source, with the exception of more nitrates. Although the presence of manganese with noncrustal particle types suggested an automotive source, it could not be justified due to the lack of diurnal and weekend−weekday variations (shown in Figure 2A,B). It is interesting to note that all the smog advisory days in summer 2002 coincide with episodes of elevated hit rates of this source (defined as the top 5% of the temporal trend), indicating a photochemically driven source. In addition, a simple principal components analysis upon the temporal trend of this source, $PM_{2.5}$ mass concentration, and local trace gas data suggested association between the organic nitrate source, ozone, and $PM_{2.5}$ mass concentration. Organic

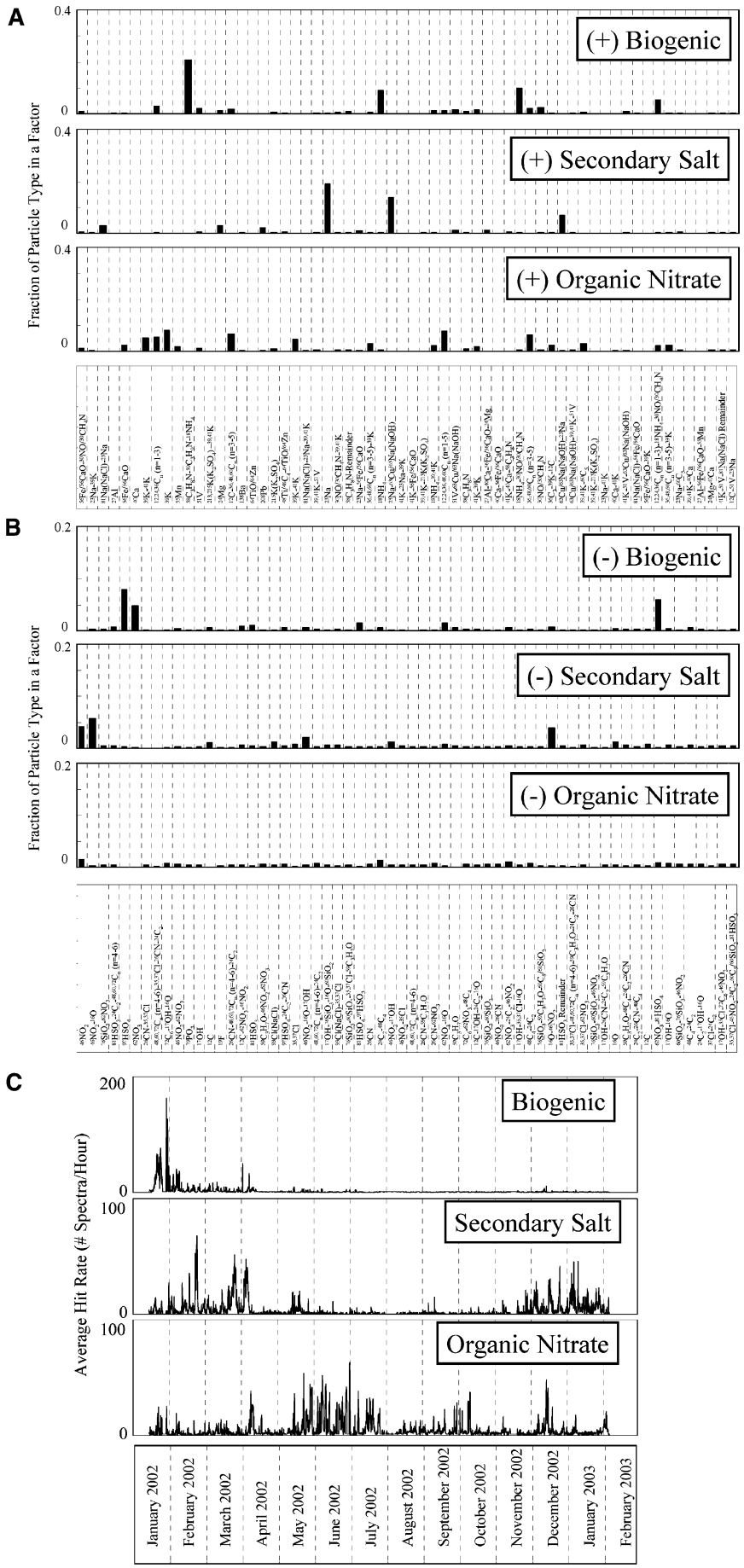

FIGURE 3. (A) Positive and (B) negative secondary source profiles and (C) secondary temporal trends for nonepisodic events.

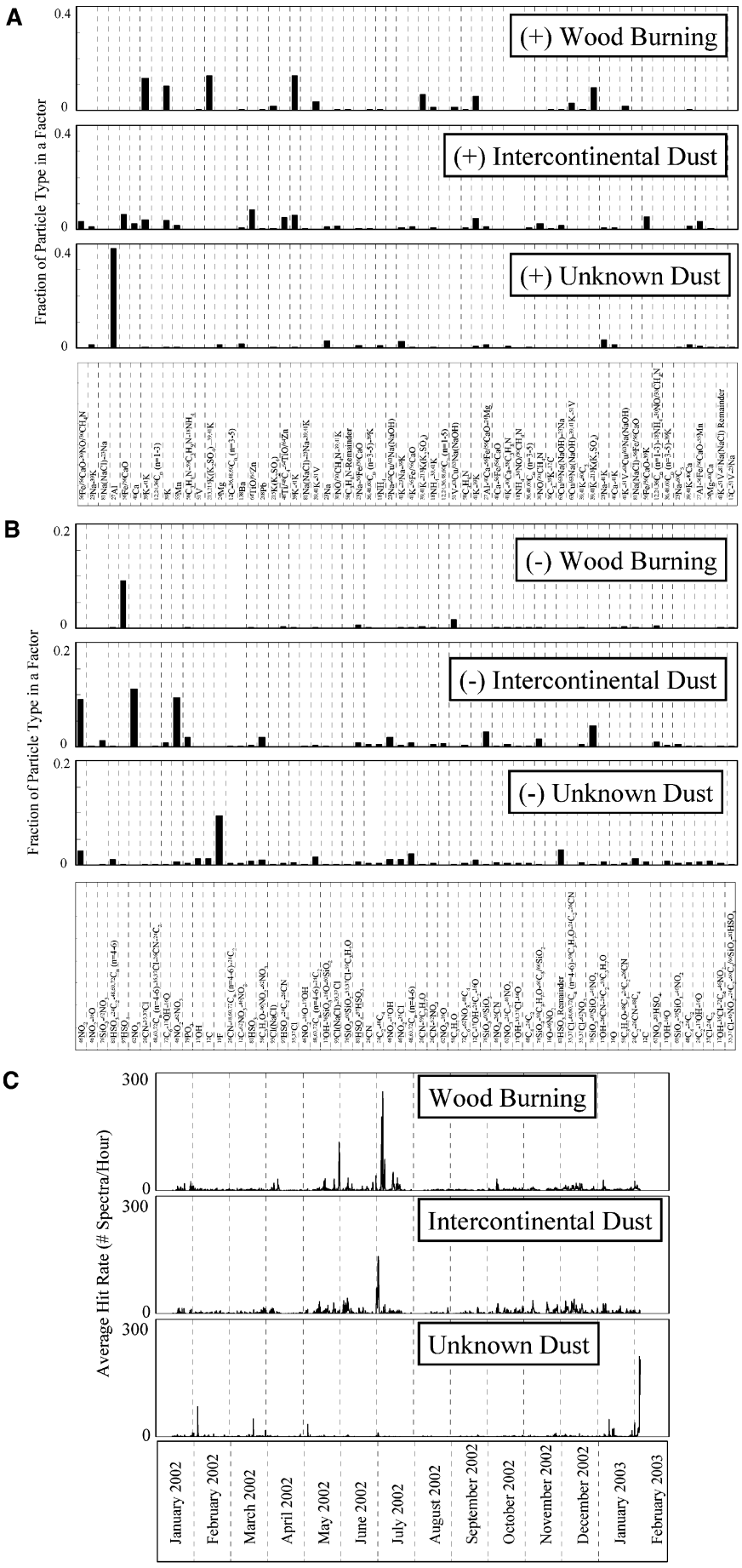

FIGURE 4. (A) Positive and (B) negative source profiles and (C) temporal trends for episodic events.

nitrates are well-known to form by the gas-phase reaction of NO_x (ozone precursors) with peroxy radicals (*31*), but their association with particulate mass has been quantified only in Los Angeles (to the best of our knowledge), where aerosol phase carbonyl content was correlated well with organic nitrates (*32*). It is thus suggested that organic nitrates may be an important particle type associated with southern Ontario smog events. Interestingly, this factor also appears for a short time on December 15, 2002, when it was markedly elevated at 8 am and 5 pm. The average temperature of this day was just over 2 °C and thus was not conducive to local photochemical production of organic PM. Furthermore, the immediately preceding and subsequent days experienced similar temperatures, and thus increased local formation of nitrate PM was not likely. It is thus suggested that this event may have been a case of long-range transport.

Source Identification of Episodic Events with PMF Receptor Modeling. By use of this nine-factor solution, three episodic events were clearly observed. For each episodic event, the positive and negative source profiles and the source temporal variation are displayed in Figure 4, panels A−C, respectively. The first factor in Figure 4 was named as a wood-burning source. Its source profile exhibited positive particle types such as potassium sulfate and potassium, and a counter negative particle type of hydrogen sulfate, common wood burning markers (*33*). The wood-burning episodes were clearly observed on June 1, 2002, July 6, 2002, and July 7, 2002. The particles from this source were thought to originate from forested areas in Quebec and the prairie provinces, regions where large fires had just occurred. Note that despite residential wood burning in Toronto during the winter, no related increase was observed in the temporal trend of this source.

The second factor in Figure 4 was named intercontinental dust. Dust particles containing crustal elements were particularly elevated on July 3, 2002. Back trajectory analysis indicated that this dust originated from Africa. Dust from the Sahara has previously been observed in the Cape Verde archipelagos and the Caribbean Sea (*34*). The positive dust particle types contained titanium, aluminum, and iron, accompanied with silicates and nitrates as their anionic counterparts. The crustal elements observed in these particles by the aerosol LAMS are known to be present in Saharan dust, although they are by no means unique to this source (*34*). Nitrate coating on these particles was not surprising as they traveled far enough for significant secondary gas−particle transformations. Since the observed particle types are frequently observed in soil, the remainder of the temporal trend may be a result of a more local dust with a similar source profile.

The last factor in Figure 4 was labeled as unknown dust that primarily exhibited a positive particle type containing aluminum with an anionic counterpart of fluoride. Aluminum smelting, coal-fired utilities, and steel production are responsible for approximately 90% of all reported releases to air of inorganic fluoride in Canada (*35*). Back trajectory analysis in February 2003 indicated that air masses arriving in Toronto during episodes of this source had not passed near any such operations. A plausible explanation, ascertained through analysis of more recent data, is that these particles emanated from construction-related grinding done with wheels composed of corundum (aluminum oxide). Work on a nearby construction project involving cutting and grinding of marble stones started at this time and continued for several months. These types of particles were observed frequently in a data set collected after the one described in the present paper.

In summary, receptor modeling by PMF on aerosol LAMS spectral data revealed nine sources that contributed to Toronto particulate matter. These were biogenic, mixed crustal, organic nitrate, construction dust, Toronto soil/road salt, secondary salt, wood burning, intercontinental dust, and an unknown aluminum fluoride source. Some of these sources contributed throughout the year, others contributed more seasonally, while three only contributed during episodic events. PMF provided reasonable source profiles for all the sources and also resolved the origins of the positive and negative particle types associated with multiple sources. Source apportionment of these sources is anticipated to be the next step. This will require scaling of the observed hit rates in order to correct for the sensitivities of different particle types and efficiency of the inlet for particles of different sizes. While scaling in order to correct for the impact of particle size on the hit efficiency is possible, correction for differences in the hit efficiency for particles of different composition remains a challenge.

Acknowledgments

We thank the Canadian Foundation for Innovation (CFI), Natural Sciences and Engineering Research Council (NSERC), Environment Canada, the Ontario Ministry of the Environment, and the Toxic Substance Research Initiative (TSRI), a research program held jointly by Health Canada and Environment Canada, for funding to construct and operate the University of Toronto Facility for Aerosol Characterization.

Literature Cited

(1) Paatero, P. Least squares formulation of robust nonnegative factor analysis. *Chemome. Intell. Lab. Syst.* **1997**, *37*, 23−35.
(2) Polissar, A. V.; Hopke, P. K.; Poirot, R. L. Atmospheric Aerosol over Vermont: Chemical Composition and Sources. *Environ. Sci. Technol.* **2001**, *35*, 4604−4621.
(3) Ramadan, Z.; Song, X. H.; Hopke, P. K. Identification of sources of Phoenix aerosol by positive matrix factorization. *J. Air Waste Manage.* **2000**, *50*, 1308−1320.
(4) Tsai, J.; Owega, S.; Evans, G.; Jervis, R.; Tan, P.; Fila, M. Chemical composition and source apportionment of Toronto summertime urban fine aerosol (PM2.5). *J. Radioanal. Nucl. Chem.* **2004**, *259*, 193−197.
(5) Xie, Y. L.; Hopke, P.; Paatero, P.; Barrie, L. A.; Li, S. M. Identification of source nature and seasonal variations of arctic aerosol by positive matrix factorization. *J. Atmos. Sci.* **1999**, *56*, 249−260.
(6) Chueinta, W.; Hopke, P. K.; Paatero, P. Investigation of sources of atmospheric aerosol at urban and suburban residential areas in Thailand by positive matrix factorization. *Atmos. Environ.* **2000**, *34*, 3319−3329.
(7) Lee, E.; Chan, C. K.; Paatero, P. Application of positive matrix factorization in source apportionment of particulate pollutants in Hong Kong. *Atmos. Environ.* **1999**, *33*, 3201−3212.
(8) Song, X.H.; Polissar, A. V.; Hopke, P. K. Sources of fine particle composition in the northeastern U.S. *Atmos. Environ.* **2001**, *35*, 5277−5286.
(9) Rhoads, K. P.; Phares, D. J.; Wexler, A. S.; et al. Size-resolved ultrafine particle composition analysis, 1. Atlanta. *J. Geophys. Res.-Atmos.* **2003** *108* (D7), art. no. 8418 JAN 21.
(10) Phares, D. J.; Rhoads, K. P.; Johnston, M. V.; et al. Size-resolved ultrafine particle composition analysis, 2. Houston. *J. Geophys. Res.-Atmos.* **2003** *108* (D7), art. no. 8420 JAN 22.
(11) Ondov, J. M. Particulate tracers for source attribution: Potential for application to California's San Joaquin Valley. *J. Aerosol Sci.* **1996**, *27*, S687−S688.
(12) Dodd, J. A.; Ondov, J. M.; Tuncel, G. Multimodal size spectra of submicrometer particles bearing various elements in rural air. *Environ. Sci. Technol.* **1991**, *25*, 890−903.
(13) Divita, F.; Suarez, A.; Ondov, J. M. Size spectra and hygroscopic growth of particles bearing As, Se, Sb and Zn in College Park aerosol. *J. Radioanal. Nucl. Chem.* **1995**, *192*, 215−228.
(14) Owega, S.; Evans, G. J.; Jervis, R. E.; Tsai, J.; Fila, M.; Tan, P. V. Comparison between urban Toronto PM and selected materials: aerosol characterization using laser ablation/ionization mass spectrometry (LAMS). *Environ. Pollut.* **2002**, *120*, 125−135.
(15) Tan, P. V.; Malpica, O.; Evans, G. J.; Owega, S.; Fila, M. Chemically assigned classification of aerosol mass spectra. *Am. Soc. Mass Spectrom.* **2002**, *13*, 826−838.

(16) Suess, D. T.; Prather, K. A. Mass spectrometry of aerosols. *Chem. Rev.* **1999**, *99*, 3007−3036.
(17) Allen, J. O.; Fergenson, D. P.; Gard, E. E.; Hughes, L. S.; Morrical, B. D.; Kleeman, M. H.; Gross, D. S.; Galli, M. E.; Prather, K. A.; Cass, G. R. Particle detection efficiencies of aerosol time-of-flight mass spectrometers under ambient sampling conditions. *Environ. Sci. Technol.* **2000**, *34*, 211−217.
(18) Qin, Y.; Oduyemi, K. Atmospheric aerosol source identification and estimates of source contributions to air pollution in Dundee, UK. *Atmos. Environ.* **2003**, *37*, 1799−1809.
(19) Larsen, R.K.; Baker, J. E. Source apportionment of polycyclic aromatic hydrocarbons in the urban atmosphere: A comparison of three methods. *Environ. Sci. Technol.* **2003**, *37*, 1873−1881.
(20) Qin, Y.; Oduyemi, K.; Chan, L. Y.; Comparative testing of PMF and CFA models. *Chemom. Intell. Lab. Syst*, **2002**, *61*, 75−87.
(21) Paatero, P.; Hopke, P. K.; Song, X.; Ramadan, Z. Understanding and controlling rotations in factor analytic models. *Chemom. Intell. Lab. Syst.* **2002**, *60*, 253−264.
(22) Oravisjarvi, K.; Timonen, K.L.; Wiikinkoski, T.; Ruuskanen, A. R.; Heinanen, K.; Ruuskanen, J. Source contributions to PM2.5 particles in the urban air of a town situated close to a steel works. *Atmos. Environ.* **2003**, *37*, 1013−1022.
(23) Fung, Y. S.; Wong, L. W. Y. Apportionment of air pollution sources by receptor models in Hong Kong. *Atmos. Environ.* **1995**, *29*, 2041−2048.
(24) Ashtek Corporation, 2002. Retrieved July 16, 2003, from http://www.ashtek.com.
(25) Tan, P. V.; Evans, G. J.; Tsai, J.; Owega, S.; Fila, M.; Malpica, O.; Brook, J. R. On-line analysis of urban particulate matter focusing on elevated wintertime aerosol concentrations. *Environ. Sci. Technol.* **2002**, *36*, 3512−3518.
(26) Angelino, S.; Suess, D. T.; Prather, K. A. Formation of aerosol particles from reactions of secondary and tertiary alkylamines: Characterization by aerosol time-of-flight mass spectrometry. *Environ. Sci. Technol.* **2001**, *35*, 3130−3138.
(27) Abalos, M.; Bayona, J. M.; Ventura, F. Development of a solid-phase microextraction GC−NPD procedure for the determination of free volatile amines in wastewater and sewage-polluted waters *Anal. Chem.* **1999**, *71*, 3531−3537.
(28) Gard, E. E.; Kleeman, M. J.; Gross, D. S.; Hughes, L. S.; Allen, J. O.; Morrical, B. D.; Fergenson, D. P.; Dienes, T.; Gaelli, M. E.; Johnson, R. J.; Cass, G. R.; Prather, K. A. Direct observation of heterogeneous chemistry in the atmosphere. *Science* **1998**, *279*, 1184−1187.
(29) Seinfeld, J. H.; Pandis, S. N. *Atmospheric Chemistry and Physics*; Wiley−Interscience: New York, 1998; p 528.
(30) Lammel, G.; Bruggemann, E.; Gnauk, T.; Muller, K.; Neususs, C.; Rohrl, A. A new method to study aerosol source contributions along the tracks of air parcels and its application to the near-ground level aerosol chemical composition in central Europe *J. Aerosol Sci.* **2003**, *34*, 1−25.
(31) Seinfeld, J. H.; Pandis, S. N. *Atmospheric Chemistry and Physics*; Wiley-Interscience: New York, 1998; p 738.
(32) Mylonas, D.; Allen, D.; Ehrman, S.; Pratsinis, S. The sources and size distributions of organonitrates in Los Angeles aerosol. *Atmos. Environ.* **1991**, *25*, 2855−2861.
(33) Silva, P. J.; Liu, D.-Y.; Noble, C. A.; Prather, K. A. Size and chemical characterization of individual particles resulting from biomass burning of local southern California species. *Environ. Sci. Technol.* **1999**, *33*, 3068−3076.
(34) Caquineau, S.; Gaudichet, A.; Gomes, L.; Legrand, M. Mineralogy of Saharan dust transported over northwestern tropical Atlantic Ocean in relation to source regions. *J. Geophys. Res.-Atmos.* **2002**, *107*, AAC 4-1−4−12.
(35) Health Canada. Canadian Environmental Protection Act, 1993. Retrieved September 2, 2003, from http://www.hc-sc.gc.ca/hecs-sesc/exsd/pdf/inorganic_fluorides.pdf.

Received for review October 22, 2003. Revised manuscript received August 5, 2004. Accepted August 11, 2004.

ES035177I